Defining Protein−Protein Interactions Using Site-Directed Spin-Labeling: The Binding of Protein Kinase C Substrates to Calmodulin†

Zhihai Qin, Stacey L. Wertz, Jaison Jacob, Yoko Savino, and David S. Cafiso*

Department of Chemistry and Biophysics Program at the University of Virginia, Charlottesville, Virginia 22901

Received July 16, 1996; Revised Manuscript Received August 26, 1996⊗

ABSTRACT: EPR spectroscopy was used to examine protein−protein interactions between calmodulin and spin-labeled peptides based on the protein kinase C substrate domains of the myristoylated alanine rich C kinase substrate (MARCKS) and neuromodulin. When bound to calmodulin, the C- and N-terminal ends of a 25 residue MARCKS derived peptide exhibited large amplitude motion on the nanosecond time scale and were accessible to paramagnetic agents in aqueous solution. However, residues 5−23 were highly protected and in contact with side chains from calmodulin. These data are consistent with an α-helical configuration for this segment of MARCKS and with structures that have been obtained for other calmodulin−substrate complexes. For the 17 residue neuromodulin derived peptide, which is Ca^{2+} independent in its binding to calmodulin, oxygen collision rates demonstrate that one helical face of this peptide interacts strongly with calmodulin. The data are consistent with an interaction of this face specifically with the C-terminal lobe of calmodulin, where this lobe is either in an "open" or "semiopen" configuration. The EPR data also indicate that the N-terminal lobe of calmodulin is in contact with the peptide, but that this lobe is not as strongly associated with the peptide target. Overall, the binding pocket for neuromodulin appears to be less compact and more dynamic than that formed by MARCKS. This behavior has not previously been seen for calmodulin substrates, and it may play a role in the Ca^{2+} independent binding of this class of substrates. This work demonstrates the utility of EPR spectroscopy to define protein−protein interactions; in addition, oxygen collision frequencies obtained at buried sites appear to provide information on the conformational dynamics of proteins.

Calmodulin (CaM)[1] is a ubiquitous calcium binding protein that functions in a wide variety of cell signaling pathways (James et al., 1995). This protein has two Ca^{2+} binding domains joined by a long flexible helix (Babu et al., 1985; Barbato et al., 1992), and it binds substrates, such as myosin light chain kinase (MLCK), by placing these two domains into contact to form a highly compact globular structure with a central pore that can accommodate a basic amphipathic α-helix (Ikura et al., 1992; Meador et al., 1992). A remarkable feature of calmodulin is its ability to bind to a wide variety of target structures. Other calmodulin targets that are high affinity and Ca^{2+} dependent in their binding are thought to interact in a manner similar to that seen for MLCK; however, the sequence requirements for strong substrate association are not strict, and this may be a result of the flexible α-helix linking the two domains (Kretsinger, 1992). In addition, several substrates such as neuromodulin are known to bind to CaM in a Ca^{2+} independent fashion (Liu & Storm, 1989); however, relatively little is known about the structures that mediate these interactions.

The myristoylated alanine rich C kinase substrate (MARCKS) (Taniguchi & Manenti, 1993) and neuromodulin are water-soluble membrane associated proteins that have been proposed to play roles in sequestering and buffering calmodulin in the nervous system (Liu & Storm, 1989; McIlroy et al., 1991). The structure of the MARCKS domain bound to CaM has not been determined, but it is one of the highest affinity CaM targets known. It is highly basic and contains 12 lysines and one arginine residue in a stretch of 25 amino acids. Although it is not as strongly amphipathic as is the binding domain of smooth muscle MLCK or the regulatory domain of the human plasma membrane Ca^{2+} ATPase, its high affinity and Ca^{2+} dependence suggest that it interacts in a manner similar to that of MLCK. For the Ca^{2+} independent substrate neuromodulin, high resolution NMR studies suggest that it also interacts as a helix (Zhang et al., 1994), but high resolution structures of this substrate/CaM complex have not yet been obtained. Peptides based on the CaM binding domain of MARCKS (McIlroy et al., 1991) or neuromodulin bind to CaM and electrostatically associate with membranes containing acid lipids, where they become substrates for PKC. Thus, they exhibit the important activities of their parent proteins.

Recent advances in resonator technology have dramatically improved the sensitivity and utility of EPR. When combined with the ability to specifically incorporate nitroxides into proteins and peptides by the use of site-directed mutagenesis or solid phase synthesis, EPR spectroscopy has become a novel and important technique to investigate the dynamics

† This work was supported by grants from the National Science Foundation (MCB-9418318) and the National Institutes of Health (GM 47525).

* All correspondence should be addressed to this author at the Department of Chemistry.

⊗ Abstract published in *Advance ACS Abstracts,* October 1, 1996.

[1] Abbreviations: CaM, calmodulin; DPPH, 2,2-diphenyl-1-picrylhydrazyl; EGTA, ethylene glycol bis(β-aminoethyl ether)-*N*,*N*,*N*′,*N*′-tetraacetic acid; EPR, electron paramagnetic resonance; IQ motif, a consensus calmodulin target having the sequence IQXXXRGXXXR; MARCKS, myristoylated alanine rich C kinase substrate; MLCK, myosin light chain kinase; MTSSL, methanethiolsulfonate spin-label; NiEDDA; nickel(II) ethylenediaminediacetic acid; NMR, nuclear magnetic resonance.

S0006-2960(96)01747-3 CCC: $12.00

and structure of proteins (Hubbell & Altenbach, 1994). Nitroxide spin-labels can be incorporated by synthesizing peptides having a single cysteine substitution followed by labeling of the peptide with a sulfhydryl-specific methanethiosulfonate spin-label MTSSL as shown below (Berliner et al., 1982). The EPR spectrum of MTSSL derivatized to cysteine is sensitive to tertiary contacts at the labeled site and to local backbone dynamics, and its incorporation is no more perturbing than other single site amino acid substitutions (Mchaourab et al., 1996).

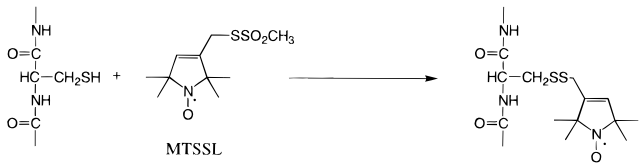

In the work described here, the CaM bound structures of the substrate domains from MARCKS and neuromodulin are investigated using site-directed spin-labeling and EPR spectroscopy. This work demonstrates that MARCKS interacts with CaM in a similar fashion to that of MLCK. Neuromodulin also interacts as a helix and appears to occupy a binding site which is similar to that of MLCK. However, only one helical face of neuromodulin associates strongly with CaM even though both lobes of CaM have closed around this target. The EPR experiments performed here demonstrate that protein−protein interactions can be defined by site-directed spin-labeling, and they provide a view of protein structure and molecular contact that may not be easily obtainable using more established structural methods.

EXPERIMENTAL PROCEDURES

Materials. Nitroxide spin-labels were incorporated into peptides derived from MARCKS and neuromodulin by synthesizing peptides having a single cysteine substitution followed by labeling the peptide with MTSSL. Spin-labeled peptides corresponding to the PKC and calmodulin binding domains of MARCKS and neuromodulin were synthesized as described previously with a Gilson Automated Multiple Peptide System synthesizer (AMS 422) using a rink amide *p*-methylbenzhydrylamine (MBHA) resin (Qin & Cafiso, 1996; Wertz et al., 1996). Mass spectrometry and HPLC were used to confirm the identity and purity of these peptides. Twelve peptides were synthesized with nitroxide labels on positions 2−5, 11−14, and 21−24 of the 25 amino acid MARCKS derived peptide corresponding to residues 151−175 of MARCKS, Ac-KKKKKRFSFKKSFKLSGFSFKKNKK-NH_2. Seventeen peptides with spin-labels on each position of the 17 residue neuromodulin derived peptide having the sequence Ac-KIQASFRGHITRKKLKG-NH_2 (Apel et al., 1990) were also produced. The methanethiosulfonate spin-label, *S*-(1-oxy-2,2,5,5-tetramethylpyrroline-3-methyl) (MTSSL) used in the synthesis was obtained from Reanal (Budapest, Hungary), and nickel(II) ethylenediaminediacetic acid (NiEDDA) used for the power saturation measurements was the generous gift of Dr. Christian Altenbach.

A highly purified grade of calmodulin from bovine brain was obtained from Calbiochem (La Jolla, CA) and was used without further purification. For this sample, neutron activation indicated that only the high affinity sites on CaM were occupied with Ca^{2+}, and samples of the neuromodulin derived peptides bound to CaM were prepared with no additional Ca^{2+}. For the neuromodulin−CaM complex, two of the labeled sites on the peptide were also examined in the presence of low or excess Ca^{2+} by the addition of either 5 mM EGTA or 5 mM Ca^{2+}. For the MARCKS derived peptides, enough Ca^{2+} was added to ensure that a large fraction of the available CaM would be fully saturated with Ca^{2+}. These samples contained peptide concentrations of 50−100 μM, with calmodulin present in excess at concentrations of 1−2 mM.

EPR Spectroscopy. EPR spectra were measured on a Varian E-line Centuries series spectrometer using an X-band loop gap resonator with a microwave power of 2 mW and a peak-to-peak modulation amplitude of 1.6 G. Quartz capillary tubes, i.d. = 0.6 mm, o.d. = 0.84 mm (Vitro Dynamics, Rockaway, NJ), were used to hold the nitroxide samples which were filled with approximately 5 μL of sample. For power saturation measurements, samples were placed in gas permeable TPX capillary tubes (Medical Advances, Milwaukee, WI), and the microwave power was increased from 0.1 to 190.0 mW, while the peak-to-peak amplitude of the $m_I = 0$ peak, $A_{m_I=0}$, was measured at regular power intervals. These power saturation data were fit to the following function:

$$A_{m_I=0} = IP^{1/2}\left[1 + (2^{1/\epsilon} - 1)\frac{P}{P_{1/2}}\right]^{-\epsilon} \quad (1)$$

where P represents the microwave power, I is a scaling factor, $P_{1/2}$ is the power required to reduce the resonance amplitude, A, to half its unsaturated value, and ϵ is a measure of the homogeneity of saturation of the resonance. In this fit, $P_{1/2}$, ϵ, and I were allowed to be adjustable parameters as described previously (Altenbach et al., 1994). Power saturation data were obtained for each sample under three different sets of conditions: equilibrated with a nitrogen atmosphere, equilibrated with air, and equilibrated with nitrogen in the presence of 20 mM NiEDDA in the aqueous phase. Values for $\Delta P_{1/2}$ were obtained from the difference in the $P_{1/2}$ values in the presence and absence of the relaxation reagents and were then used to estimate the relative collisional rates between nitroxides and selected paramagnetic species using the following equation:

$$\Pi = \frac{\Delta P'_{1/2}}{P'_{1/2}(\mathrm{DPPH})} \quad (2)$$

Here, Π is the collision parameter, $\Delta P'_{1/2}$ is the value of $\Delta P_{1/2}$ divided by the peak-to-peak linewidth of the central $m_I = 0$ resonance, and $P'_{1/2}$ is the value of $P_{1/2}$ for solid DPPH divided by its linewidth (Altenbach et al., 1990; Farahbakhsh et al., 1992).

RESULTS AND DISCUSSION

The MARCKS−CaM Interaction Resembles That of MLCK-CaM. Shown in Figure 1 are 12 EPR spectra corresponding to spin-labels derivatized to positions 2−5, 11−14, and 21−24 of the 25 amino acid peptide MARCKS derived peptide. There is an excess of Ca^{2+}/CaM present in these samples, and in each case the peptides are completely bound to CaM. In several spectra, small narrow features that are seen at the high field resonance position are due to a minor impurity of unattached nitroxide in solution. At positions 2 and 3, the EPR lineshapes are relatively narrow, indicating that there

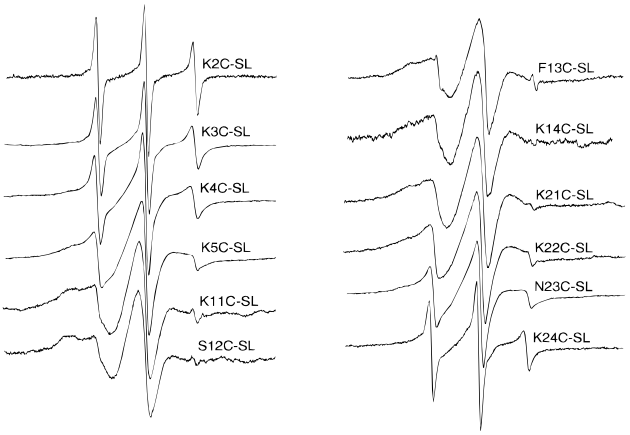

FIGURE 1: EPR spectra obtained for spin-labeled derivatives of a MARCKS derived peptide bound to CaM. Single nitroxide substitutions were incorporated into positions 2−5, 11−14, and 21−24. Peptides were mixed at concentrations of 50−100 μM with CaM at concentrations of approximately 1 mM in a solution containing 100 mM NaCl and 1.0 mM Ca^{2+} at pH = 7.0. Spectra were recorded using an X-band loop gap resonator with a microwave power of 2 mW and a modulation amplitude of 1 G p-p.

are large amplitude motions on the nanosecond time scale. The MARCKS derived peptide assumes an extended structure in solution (Qin & Cafiso, 1996), and a reasonable interpretation of these lineshapes is that this end of the peptide either has no secondary structure or is highly dynamic when bound to CaM. At positions 4 and 5 the motion of the label is much more anisotropic, suggesting that the side chain and/or the backbone of the peptide is being constrained by its interaction with CaM. Spectra for labels at positions 11−14 are quite broad and are consistent with spectra that are obtained for labels buried within a protein and undergoing strong tertiary interactions with other residues (Mchaourab et al., 1996). At the C-terminal end, positions 21−24 show successively increased amplitudes of motion. The spectra demonstrate that the middle portion of the peptide is interacting strongly with CaM, with the N- and C-termini exhibiting a relatively high degree of motion.

These spectra can be examined in a more quantitative fashion by plotting the reciprocal of the central $m_I = 0$ linewidth (ΔH_0^{-1}) as shown in Figure 2A. For the label used here, values of ΔH_0^{-1} greater than 0.35 G^{-1} are generally associated with labels on the exposed surface of proteins, either on a helix or in a loop region, while values less than 0.3 are associated with labels undergoing strong tertiary contact with protein side chains (Mchaourab et al., 1996). These linewidth data indicate that the ends of the peptide are exposed to solution, while residues in the central portion of the peptide are experiencing some tertiary contact.

Shown in Figure 2B are the collision parameters (Π) for NiEDDA and O_2 as a function of the position of the spin-label on the MARCKS peptide when it is associated with CaM. The value of Π is determined using CW power saturation, and it provides a measure of the relative collisional rate of the paramagnetic reagent with the spin-label (Altenbach et al., 1990; Farahbakhsh et al., 1992). Both reagents show similar collision profiles, and spin-labels from residues 5−23 appear to be protected from these paramagnetic species upon binding to CaM. Spin-labels at the C- and N-termini freely undergo collisions with these reagents and yield values of Π that are similar to those obtained for water-soluble nitroxides. It can be seen for the MARCKS peptide that the collision accessibility reflects the mobility pattern seen in Figures 1 and 2A. From Figure 2A, residues 5−21 appear to be in strong tertiary contact with CaM. This is consistent with the binding pocket for MLCK determined by X-ray diffraction and by NMR (Ikura et al., 1992; Meador et al., 1992). In the NMR structure of Ca^{2+}/CaM/skeletal MLCK a tryptophan at position 4 and a phenylalanine at position 17 define the N- and C-terminal ends of a peptide from MLCK that interact with CaM. MARCKS has phenylalanines in positions 7 and 20, and the collision profiles in Figure 2B suggest a similar binding motif for MARCKS to CaM.

Neuromodulin Forms Specific Contacts with One CaM Lobe. EPR spectra for spin-labeled peptides corresponding to the CaM and PKC binding domain of neuromodulin, residues 37−53, bound to CaM were obtained. Several of these spectra along with the reciprocal of the linewidth of the central nitroxide resonance (ΔH_0^{-1}) for each labeled peptide are shown in Figure 3. Figure 3 shows spectra for positions 5−9 and 17 which are representative of the spectra found for the 17 neuromodulin derived peptides. Most of the spectra resemble those shown for positions 5−9. They are highly anisotropic and characteristic of nitroxides undergoing tertiary interactions with the CaM structure. However, at the ends of the peptide, positions 2, 15, and 17 yield spectra that are much more isotropic as seen in Figure 3 for G17C-SL. At these positions, the values of ΔH_0^{-1} are high, suggesting that the nitroxides are exposed on the surface of the neuromodulin−CaM complex. Thus, except at the ends of the peptide, nitroxides in most positions appear to be in strong tertiary contact with CaM.

Shown in Figure 4 are the collision parameters for NiEDDA and O_2 for the neuromodulin derived peptide bound to CaM. Compared to MARCKS, a smaller segment of the neuromodulin domain is protected from NiEDDA by its binding site on CaM. For residues 2, 15, and 17, the nitroxide is highly accessible to NiEDDA, consistent with the linewidth data shown in Figure 3. However, unlike the MARCKS derived peptide, the collision parameters for NiEDDA and O_2 show distinctly different patterns. From positions 3 to 12, NiEDDA has a low accessibility to the labeled peptide with values similar to that for the protected domain of MARCKS; however, for O_2 the collision parameter exhibits an oscillatory behavior in this stretch of the peptide with an α-helical frequency. The oxygen accessibility is higher in this protected domain of neuromodulin compared to the protected domain in the MARCKS−CaM complex. Thus, the NM derived peptide apparently binds as an α-helix to CaM, where O_2 has access to one face of the helix. The lower oxygen collision parameters for positions 5, 8, and 12 suggests that these positions are buried into a binding site on CaM. When the value of ΠO_2 was examined for positions 7 and 8 in the presence of either EGTA or Ca^{2+}, no significant change in the collision parameter for oxygen was found. Thus, at least for these two positions ΠO_2 is independent of the Ca^{2+} level.

Previous work has shown that the largest chemical shifts upon neuromodulin binding to CaM occur within the C-terminal lobe (Urbauer et al., 1995), and we propose that the C-terminal lobe interacts with the surface of the helix defined by positions 5, 8, and 12. The higher O_2 accessibility for the opposite surface of the helix indicates that the binding pocket for this peptide is not completely closed as is the binding pocket surrounding MARCKS.

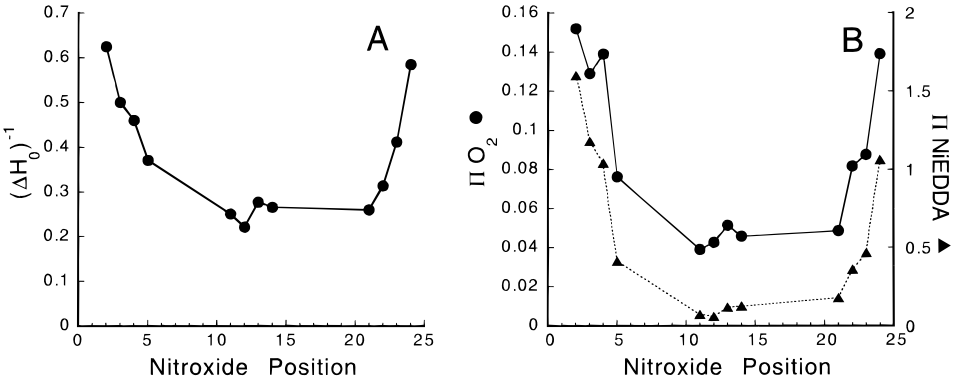

FIGURE 2: (A) Reciprocal of the central nitroxide resonance linewidth (ΔH_0^{-1}), plotted as a function of the nitroxide position. (B) The accessibility parameter Π versus label position for MARCKS derived peptides bound to CaM. This parameter provides a measure of the relative frequency of collisions of paramagnetic species Ni(II)EDDA (▲) and O_2 (●) with the indicated nitroxide-labeled peptide. Power saturation data for the spectra shown in Figure 1 were obtained in the presence of 20 mM NiEDDA, or air. The parameter Π was determined as described previously (Farahbakhsh et al., 1992).

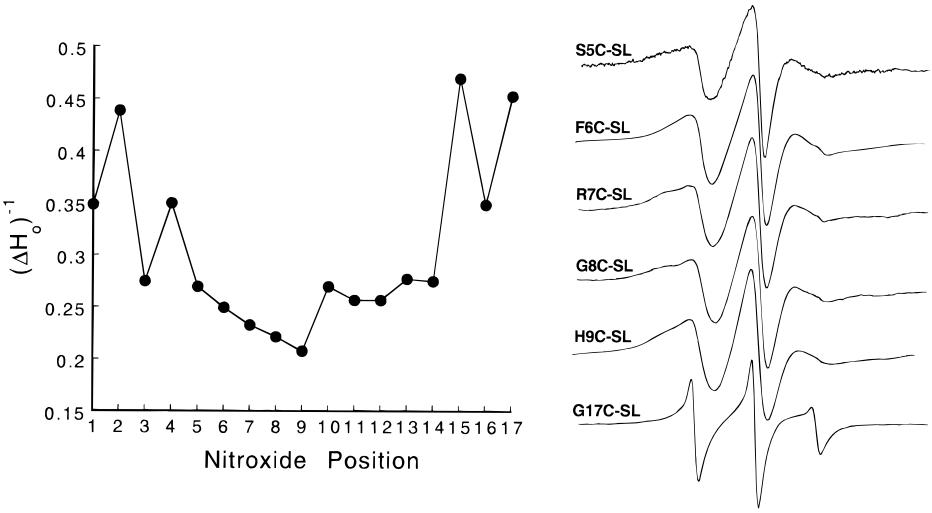

FIGURE 3: The reciprocal of the peak-to-peak linewidth of the central nitroxide resonance (ΔH_0^{-1}) in units of G^{-1} for 17 neuromodulin derived peptides bound to CaM as a function of the nitroxide position. Also shown are representative EPR spectra for nitroxides at positions 5−9 and 17 of the neuromodulin peptide when bound to CaM. The samples contain approximately 50 μM peptide in the presence of 1 mM calmodulin in a solution of 100 mM KCl and 1 mM MOPS, pH = 7.0.

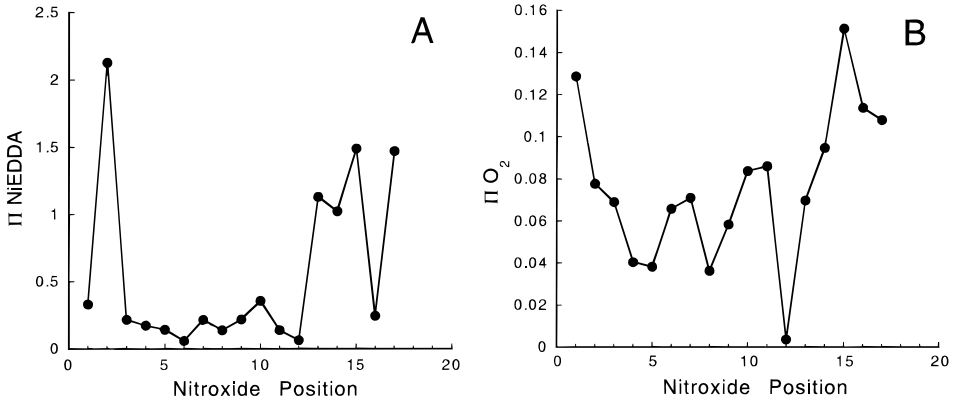

FIGURE 4: The accessibility parameter Π versus label position for the 17 neuromodulin derived peptides bound to CaM. Power saturation data were obtained for EPR spectra of each NM derived peptide in the presence of (A) 20 mM NiEDDA or (B) Air. The collision parameter, Π, was calculated as described previously (Farahbakhsh et al., 1992).

Model for the Binding of Neuromodulin to CaM. To determine whether the collision parameters for oxygen are consistent with likely CaM/substrate structures, the neuromodulin derived peptide was docked as an α-helix to uncomplexed CaM using Affinity (Stouten et al., 1993; Luty et al., 1995). This peptide docked best with the C-terminal domain as shown in Figure 5, yielding a structure that was consistent with the exposure to O_2 seen in Figure 4B. In this orientation a lysine residue at position 14 on the neuromodulin derived peptide forms an ion pair with Glu 127 in a pocket on CaM. This is the most favorable orientation for the neuromodulin helix, and it is consistent with orientations found for other CaM/peptide substrates. The C-terminal lobe shown in Figure 5 is sometimes referred to as an "open" lobe structure, but pairs of EF hands which make up these Ca^{2+} binding lobes have also been observed

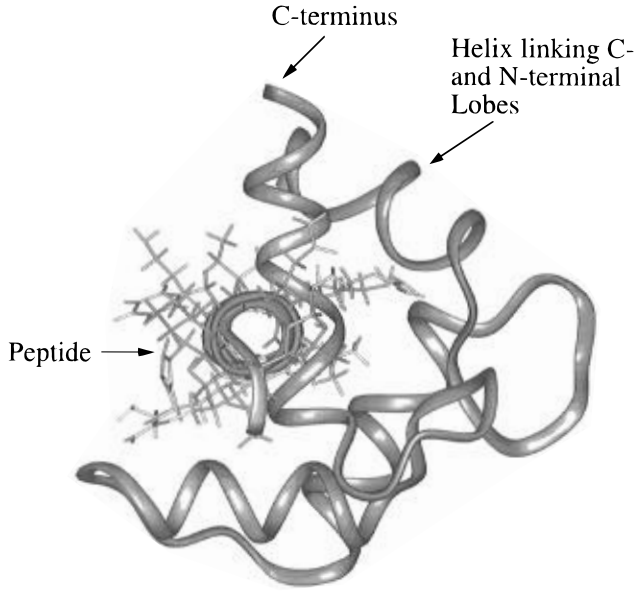

FIGURE 5: Proposed binding site for the neuromodulin derived peptide bound to calmodulin. Beginning with the unoccupied CaM crystal structure (Babu et al., 1985), the NM bound peptide in an α-helical configuration was docked to the C-terminal domain of CaM in a manner that placed positions 5, 8, and 12 in a grove in this domain, consistent with the ΠO_2 data. In the orientation shown, a salt bridge is formed between the peptide and CaM. The Π NiEDDA and ΔH_0^{-1} data indicate that the N-terminal lobe must be in close proximity to the face of the helix that shows some exposure to O_2.

in "semiopen" or "closed" conformations (Houdusse & Cohen, 1995). This peptide could be docked with the "semiopen" conformation of the C-terminal lobe in the apocalmodulin structure (Zhang et al., 1995) and also yielded contacts that were qualitatively consistent with the ΠO_2 data. A more quantitative analysis of the data may allow these forms to be distinguished.

Figure 5 does not show the N-terminal lobe, which must also be in contact with the substrate target. The neuromodulin derived peptide cannot be exposed on one face as this would not be consistent with either the low exposure of NiEDDA or the lack of helical periodicity in the EPR linewidths (see Figure 3). Because O_2 and NiEDDA are dramatically different in size, we speculate that incomplete closing of both lobes of CaM around the substrate and dynamic fluctuations of one CaM lobe relative to the other allows O_2, but not NiEDDA, access to one face of the neuromodulin helix. Thus, O_2 collision frequencies at these buried spin-labeled sites appear to reflect the dynamics of this CaM−substrate complex. The interactions of this peptide substrate with CaM may be stabilized by interactions from both lobes of CaM; however, the peptide appears to be strongly associated only on one face. This picture appears to be different than that of the essential light chain of myosin, where the first half of the IQ motif interacts with the C-terminal lobe and the second half of the motif interacts with the N-terminal lobe (Houdusse & Cohen, 1995).

It should be noted that the C-terminal lobe of CaM has two high-affinity Ca^{2+} binding sites that are normally occupied in the cell cytoplasm. The data shown here suggest that the neuromodulin derived peptide fails to make strong specific contacts with the opposite, N-terminal, lobe, a feature that may in part account for the Ca^{2+} independence in the binding of this protein. The N-terminal lobe becomes occupied at higher cellular levels of Ca^{2+} and is an event that normally leads to the binding of substrates such as MLCK and MARCKS.

All the spin-labeled peptides that were examined here bound to CaM. The fact that the placement of these labels did not significantly diminish the ability of these peptides to associate with CaM is consistent with the observations made in T4 lysozyme where nitroxides were found to be no more perturbing than other single site changes (Mchaourab et al., 1996). This work demonstrates the utility of site-directed nitroxide labeling to define both the structure and dynamics of protein−protein interactions. EPR spectroscopy provides a window on protein dynamics that may not be easily accessible using other techniques, and it is equally applicable to high molecular weight species or membrane bound proteins where techniques such as NMR and X-ray diffraction have more limited utility.

ACKNOWLEDGMENT

We would like to thank Prof. Robert Kretsinger for many helpful comments and reading of the manuscript.

REFERENCES

Altenbach, C., Marti, T., Khorana, G., & Hubbell, W. (1990) *Science 248*, 1088−1092.
Altenbach, C., Greenhalgh, D. A., Khorana, H. G., & Hubbell, W. L. (1994) *Proc. Natl. Acad. Sci. U.S.A. 91*, 1667−1671.
Apel, E. D., Byford, M. F., Au, D., Walsh, K. A., & Storm, D. R. (1990) *Biochemistry 29*, 2330−2335.
Babu, Y. S., S., S. J., Greenhough, T. J., Bugg, C. E., Means, A. R., & J., C. W. (1985) *Nature 315*, 37−40.
Barbato, G., Ikura, M., Kay, L. E., Pastor, R. W., & Bax, A. (1992) *Biochemistry 31*, 5269−5278.
Berliner, L. J., Grinwald, J., Hankovszky, H. O., & Hideg, K. (1982) *Anal. Biochem. 119*, 450−455.
Farahbakhsh, Z. T., Altenbach, C., & Hubbell, W. L. (1992) *Photochem. Photobiol. 56*, 1019−1033.
Houdusse, A., & Cohen, C. (1995) *Proc. Natl. Acad. Sci. U.S.A. 92*, 10644−10647.
Hubbell, W. L., & Altenbach, C. (1994) *Curr. Opin. Struct. Biol. 4*, 566−578.
Ikura, M., Barbato, G., Klee, C. B., & Bax, A. (1992) *Cell Calcium 13*, 391−400.
James, P., Vorherr, T., & Carafoli, E. (1995) *Trends Biochem. Sci. 20*, 38−42.
Kretsinger, R. H. (1992) *Science 258*, 50−51.
Liu, Y., & Storm, D. R. (1989) *J. Biol. Chem. 264*, 12800−12804.
Luty, B. A., Wasserman, Z. R., Stouten, P. F. W., Hodge, C. N., Zacharias, M., & McCammon, J. A. (1995) *J. Comput. Chem. 16*, 454−464.
Mchaourab, H., Lietzow, M., Hideg, K., & Hubbell, W. (1996) *Biochemistry 35*, 7692−7704.
McIlroy, B. K., Walters, J. D., Blackshear, P. J., & Johnson, J. D. (1991) *J. Biol. Chem. 266*, 4959−4964.
Meador, W. E., Means, A. R., & Quiocho, F. A. (1992) *Science 257*, 1251−1255.
Qin, Z., & Cafiso, D. S. (1996) *Biochemistry 35*, 2917−2925.
Stouten, P. F. W., Froemmel, C., Nakamura, H., & Sander, C. (1993) *Mol. Simulation 10*, 97−120.
Taniguchi, H., & Manenti, S. (1993) *J. Biol. Chem. 268*, 9960−9963.
Urbauer, J. L., Short, J. H., Dow, L. K., & Wand, A. J. (1995) *Biochemistry 34*, 8099−8109.
Wertz, S. L., Savino, Y., & Cafiso, D. S. (1996) *Biochemistry 35*, 11104−11112.
Zhang, M., Vogel, H. J., & Zwiers, J. (1994) *Biochem. Cell Biol. 72*, 109−116.
Zhang, M., Tanaka, T., & Ikura, M. (1995) *Nature, Struct. Biol. 2*, 758−767.

BI961747Y